Reprinted from

Journal of Organometallic Chemistry

Journal of Organometallic Chemistry 494 (1995) 169–177

Synthesis, characterization, reactivity, and catalytic hydrogenation activity of the hexanuclear hexahydrido carbonyl cluster compound $[Ru_6(\mu\text{-}H)_6(\mu_3,\eta^2\text{-ampy})_2(CO)_{14}]$ (Hampy = 2-amino-6-methylpyridine)

Javier A. Cabeza *, Ignacio del Río, José M. Fernández-Colinas, Angela Llamazares, Víctor Riera

Instituto de Química Organometálica, Facultad de Química, Universidad de Oviedo, 33071 Oviedo, Spain

Received 26 October 1994

ELSEVIER

ELSEVIER

Journal of Organometallic Chemistry 494 (1995) 169–177

Journal of Organometallic Chemistry

Synthesis, characterization, reactivity, and catalytic hydrogenation activity of the hexanuclear hexahydrido carbonyl cluster compound $[Ru_6(\mu\text{-}H)_6(\mu_3,\eta^2\text{-ampy})_2(CO)_{14}]$ (Hampy = 2-amino-6-methylpyridine)

Javier A. Cabeza *, Ignacio del Río, José M. Fernández-Colinas, Angela Llamazares, Víctor Riera

Instituto de Química Organometálica, Facultad de Química, Universidad de Oviedo, 33071 Oviedo, Spain

Received 26 October 1994

Abstract

The reaction of the 48-electron complex $[Ru_3(\mu\text{-}H)(\mu_3,\eta^2\text{-ampy})(CO)_9]$ (**1**) (Hampy = 2-amino-6-methylpyridine) with molecular hydrogen (1 atm, toluene, 110°C) gives the 92-electron hexanuclear hexahydrido derivative $[Ru_6(\mu\text{-}H)_6(\mu_3,\eta^2\text{-ampy})_2(CO)_{14}]$ (**2**). This hexanuclear compound regenerates complex **1** when exposed to carbon monoxide. However, it undergoes CO substitution instead of ligand addition when treated with PR_3 to give $[Ru_6(\mu\text{-}H)_6(\mu_3,\eta^2\text{-ampy})_2(PR_3)_2(CO)_{12}]$ (R = 4-tolyl (**3a**) or Ph (**3b**)). The X-ray diffraction structure of **3a** indicates that it consists of two trinuclear fragments connected to each other through two bridging hydrides, and two weak metal–metal bonds. NMR experiments (^1H, ^{13}C, homonuclear ^1H NOE, and heteronuclear indirect ^{13}C–^1H correlations) indicate that **2** is isostructural with **3a**. Complex **2** is an efficient catalyst precursor for the homogeneous hydrogenation of unsaturated organic molecules. A kinetic analysis of the hydrogenation of diphenylacetylene under very mild conditions (T = 323 K, $P(H_2) < 1$ atm) has shown that the reaction is first-order in the concentration of **2**, first-order in hydrogen pressure and zero-order in substrate concentration, suggesting that the active catalytic species are hexanuclear.

Keywords: Ruthenium; Hydride; Cluster; X-ray structure; Catalytic hydrogenation; Alkyne hydrogenation kinetics

1. Introduction

During the last two decades, the chemistry of transition metal cluster complexes has received considerable attention. Intense research activity has revealed that many of these polynuclear complexes not only have very interesting structural aspects and new reactivity patterns [1], but also a high catalytic activity when they are used as catalyst precursors in a variety of transformations of organic substrates [2]. However, in spite of the great deal of data now available, most of the new reactions in which transition metal cluster complexes are involved are still very far from being predictable.

Prompted by the fact that the cluster complex $[Ru_3(\mu\text{-}H)(\mu_3,\eta^2\text{-ampy})(CO)_9]$ (**1**) (Hampy = 2-amino-6-methylpyridine) is an efficient catalyst precursor for the homogeneous hydrogenation of alkynes to alkenes and of dienes to monoenes [3], we studied its stoichiometric reaction with molecular hydrogen. This reaction led unexpectedly to the 92-electron hexanuclear hexahydrido carbonyl cluster complex $[Ru_6(\mu\text{-}H)_6(\mu_3,\eta^2\text{-ampy})_2(CO)_{14}]$ (**2**) [4]. We now report full details of the synthesis, characterization, reactivity and catalytic hydrogenation activity of this unusual hexanuclear cluster compound. Part of this work has been published in a preliminary form [4].

2. Results and discussion

2.1. Synthesis, characterization and reactivity studies

The reaction of $[Ru_3(\mu\text{-}H)(\mu_3,\eta^2\text{-ampy})(CO)_9]$ (**1**) with dihydrogen (1 atm, toluene, reflux temperature, 75 min) gives $[Ru_6(\mu\text{-}H)_6(\mu_3,\eta^2\text{-ampy})_2(CO)_{14}]$ (**2**) (Scheme 1). This reaction is reversible in the sense that **2** reacts with carbon monoxide (1 atm, toluene or THF, room temperature) regenerating complex **1**.

* Corresponding author.

SSDI 0022-328X(94)05372-3

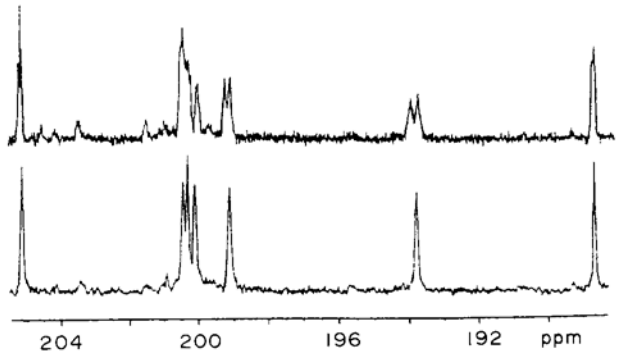

Fig. 1. Proton coupled (top) and proton decoupled (bottom) ^{13}C NMR spectra of compound **2** in the carbonyl region (THF-d_8).

The structural characterization of compound **2** proved to be very troublesome. Its IR spectrum is uninformative, because only bands from the ampy and terminal CO ligands are observed. Its ^1H NMR spectrum shows three hydrido signals which couple to each other with small coupling constants (less than 2 Hz) apart from the ampy resonances. The $^{13}C\{^1H\}$ NMR spectrum of a ^{13}CO-enriched sample in THF-d_8, shows seven resonances in the carbonyl region, all of similar intensity (only six peaks, one of higher intensity than the rest, are observed when the spectrum is run in CD_2Cl_2). In the proton-coupled ^{13}C NMR spectrum (Fig. 1), resonances at δ 200.1, 199.1 and 193.8 significantly split indicating that only three CO ligands are approximately *trans* to hydrido ligands [5]. No FAB mass spectrum and no single crystals of this compound could be obtained, probably because of its low solubility.

These data were not enough to assign precisely a structure to this compound, and in order to obtain crystals of one of its derivatives suitable for an X-ray diffraction study, its reactivity was studied. Unfortunately, although **2** proved to be very reactive (it reacts at room temperature with phosphines, nitriles, isonitriles, alkynes), most of its reactions led to complex mixtures of compounds, and only in the case of triarylphosphines were we able to isolate pure products.

The compounds $[Ru_6(\mu\text{-}H)_6(\mu_3,\eta^2\text{-ampy})_2(PR_3)_2(CO)_{12}]$ (R = 4-tolyl (**3a**) or Ph (**3b**)) were obtained from the reactions of complex **2** with tri-4-tolyl- and triphenyl-phosphine (Scheme 1). Their IR and NMR (^1H, ^{13}C, ^{31}P) spectra indicate that both compounds are isostructual, but are not very informative as to structure.

Fortunately, the structure of the compound **3a** · $2CH_2Cl_2$ could be determined by X-ray diffraction methods (Fig. 2, Table 1). The cluster consists of two symmetry-related (inversion centre) trinuclear units in which the ampy fills three axial sites (the dihedral angle between the planes defined by the pyridine ring and the metallic triangle is 86.5(4)°). Each trinuclear unit contains six CO (three in axial sites, *trans* to the nitrogen atoms, and three in equatorial sites) and one phosphine (in an equatorial site, *cis* to the pyridine nitrogen atom). The ligand shell of each trinuclear unit is completed by three hydrides. Two of them, H(1) and H(2), interact with only two ruthenium atoms (H(1) is coplanar with the metallic triangle, but the planes H(2)–Ru(2)–Ru(3) and Ru(1)–Ru(2)–Ru(3) define a dihedral angle of 80(3)°), whereas the hydride H(3) interacts with at least three ruthenium atoms (Ru(2), Ru(3) and Ru(2′)). Although the presence of metal–metal bonds between both Ru_3 units cannot be completely ruled out, these interactions have to be weak, because the distances Ru(2)–Ru(2′), Ru(2)–Ru(3′) and Ru(3)–Ru(3′) (Table 1) are

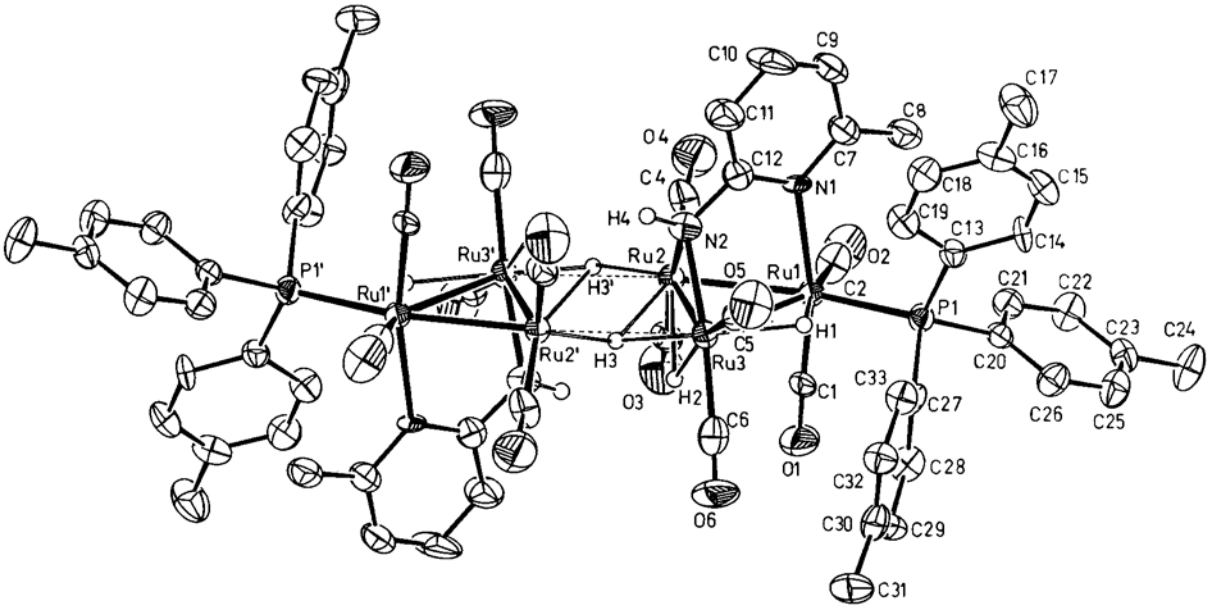

Fig. 2. Molecular structure of complex **3a** (40% thermal ellipsoids). The primed atoms are related to the unprimed by an inversion centre.

Table 1
Selected interatomic distances (Å) and angles (°) in **3a**·$2CH_2Cl_2$ [a]

Ru(1)–Ru(2)	2.724(2)	Ru(1)–Ru(3)	2.991(2)
Ru(2)–Ru(3)	2.799(2)	Ru(2)–Ru(2′)	4.266(3)
Ru(2)–Ru(3′)	3.292(3)	Ru(3)–Ru(3′)	4.376(5)
Ru(1)–N(1)	2.211(9)	Ru(2)–N(2)	2.13(1)
Ru(3)–N(2)	2.14(1)	Ru(1)–P(1)	2.395(4)
Ru(1)–C(1)	2.85(2)	Ru(1)–C(2)	1.89(1)
Ru(2)–C(3)	1.88(2)	Ru(2)–C(4)	1.88(1)
Ru(3)–C(5)	1.89(1)	Ru(3)–C(6)	1.93(2)
H(1)–Ru(1)	1.9(1)	H(1)–Ru(3)	1.92(7)
H(2)–Ru(2)	2.0(1)	H(2)–Ru(3)	2.0(1)
H(3)–Ru(2)	2.2(1)	H(3)–Ru(3)	1.9(1)
H(3)–Ru(2′)	2.3(1)	H(3)–Ru(3′)	2.6(1)
Ru(1)–Ru(2)–Ru(3)	65.50(1)	Ru(1)–Ru(3)–Ru(2)	56.00(1)
Ru(2)–Ru(1)–Ru(3)	58.40(1)	Ru(2)–Ru(1)–P(1)	162.2(1)
N(1)–Ru(1)–P(1)	96.6(3)	Ru(2)–N(2)–Ru(3)	82.0(4)

[a] Symmetry code for primed atoms: $-x, -y, -z$.

much longer than is normally expected for a Ru–Ru single bond [6]. Therefore, each trinuclear unit can be considered as an unsaturated 46-electron fragment.

Subsequent NMR experiments (^{1}H NOE and ^{13}C-^{1}H correlations) demonstrated that complex **2** is isostructural with its phosphine-substituted derivatives **3a** and **3b**. In particular, the hexanuclear structure of complex **2** was clearly established by ^{1}H NOE difference experiments (Fig. 3). Because the molecule is a symmetric dimer, selective presaturation of the amide H(4) proton resonance affords positive NOE enhancements of the hydride H(2) and H(3) signals (the unprimed atoms cannot be distinguished from the primed ones by NMR experiments; numbering as for complex **3a** in Fig. 2), whereas were **2** trinuclear, presaturation of the amide proton resonance would never result in positive enhancement of more than one hydrido signal [7]. Comparable conclusions can be drawn from the ^{1}H NOESY spectrum of complex **3a** (Fig. 4), in which it is clearly seen that H(4) is related to the hydrides H(2) and H(3), but not to H(1).

Therefore, the hydrogenation of complex **1** seems to imply oxidative addition of dihydrogen to a trinuclear 48-electron carbonyl cluster complex and the displacement of two CO to give an unsaturated 46-electron species which is stabilised via dimerization to give

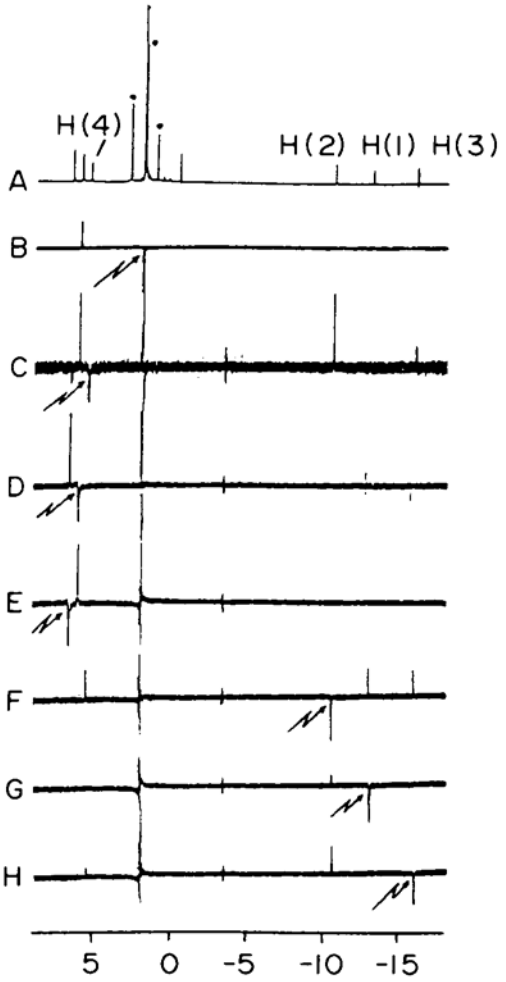

Fig. 3. (A) ^{1}H NMR spectrum of complex **2** in THF-d_8. The marked peaks correspond to impurities (water or residual THF). (B)–(H) NOE-difference spectra after selective presaturation at the indicated frequencies.

complex **2**. This reaction can be compared to that of $[Os_3(CO)_{12}]$ with dihydrogen, but in that case the unsaturated 46-electron species $[Os_3(\mu\text{-}H)_2(CO)_{10}]$ is stable [8]. This type of reaction, which is novel in ruthenium chemistry, may have significance in homogeneous catalytic hydrogenation processes involving carbonyl cluster complexes. It should also be noted that **2**, **3a**, and

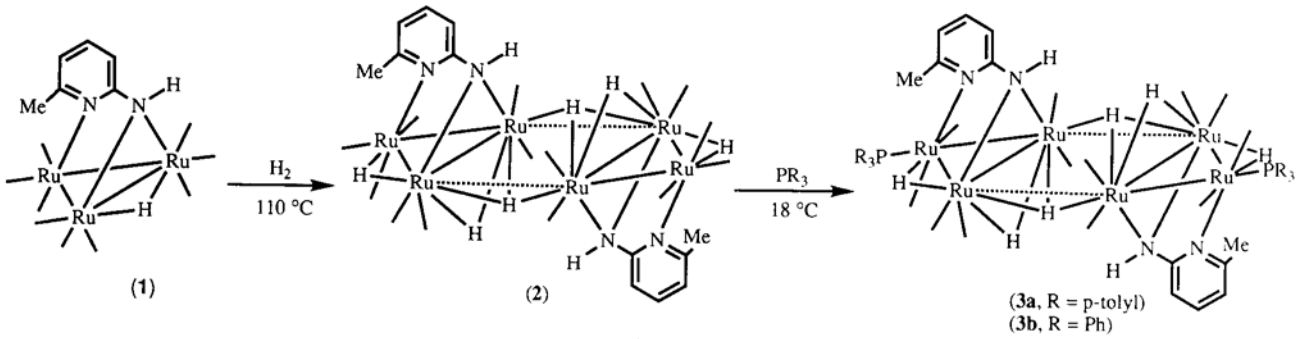

Scheme 1.

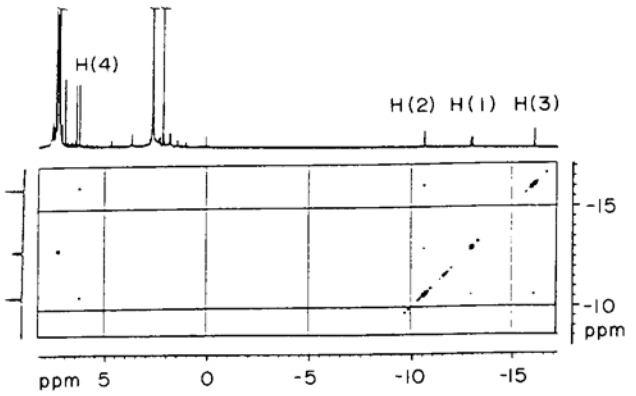

Fig. 4. A fragment of the ^{1}H NOESY spectrum of complex **3a** ($CDCl_3$).

3b, which consist essentially of two 46-electron fragments linked by hydrides, represent a unique type of compound in the chemistry of the transition metals and that unsaturated 46-electron cluster complexes are very rare. To date, only one such unsaturated ruthenium compound has been isolated [$Ru_3(\mu$-H)(μ-PPh_2)$(CO)_9$] [9], and it has a rich derivative chemistry [10] and an interesting catalytic activity [11].

2.2. Catalytic hydrogenation studies

Complex **2** is a catalyst precursor for the homogeneous hydrogenation of unsaturated organic molecules under mild conditions. Table 2 shows the results obtained at three different dihydrogen pressures, after 30 min at 353 K, for a variety of substrates. Apart from 1,5-cyclooctadiene and 1,3-cyclohexadiene, which could be efficiently hydrogenated at 2.2 atm, and diphenylacetylene, which was easily converted into a mixture of *cis*- and *trans*-stilbene at 1 atm, all of the other substrates required longer reaction times and/or higher dihydrogen pressures to be hydrogenated conveniently.

At this point, it should be noted that although many mechanisms of homogeneous reactions catalyzed by mononuclear transition-metal complexes are now well known [12], very few mechanisms of homogeneous reactions catalyzed by transition-metal cluster compounds have been determined [2,12,13]. In a few cases, the catalyst precursors change their nuclearity during cluster-promoted catalytic reactions [2,14], but in most of the catalytic reactions in which cluster compounds are involved the fate of the catalytic precursors has not been investigated [2].

The fact that diphenylacetylene was hydrogenated under very mild conditions in the presence of complex **2** (Fig. 5), prompted us to carry out a kinetic study of this catalytic reaction. As shown in Fig. 5, *cis*-stilbene is the kinetic product and *trans*-stilbene is the thermodynamic product, because the *cis*- to *trans*-stilbene ratio decreases continuously as the hydrogenation of the alkyne progresses. Hydrogenation of stilbene to 1,2-diphenylethane was not observed, even at high conversions. As there are two reactions competing for the same catalyst, the hydrogenation of diphenylacetylene to *cis*-stilbene and the isomerization of the latter into *trans*-stilbene, and as no isomerization is observed in the initial stages of the reaction, our kinetic studies were carried out using data of the initial 10 min of each run.

Hydrogenation rates were obtained at 323 K by measuring the dihydrogen uptake as a function of time, and correcting the observed volume of consumed dihydrogen to that corresponding to 1 atm. In order to

Table 2
Results of the catalytic hydrogenation of several unsaturated organic substrates promoted by complex **2** [a]

Substrate	$P(H_2)$ = 15 atm	$P(H_2)$ = 2.2 atm	$P(H_2)$ = 1 atm
1,3-Cyclohexadiene		cyclohexene (100%)	substrate (94.9%) cyclohexene (5.1%)
1,5-Cyclooctadiene		cis-cyclooctene (73.1%) cyclooctane (26.9%)	substrate (4.3%) 1,3-cyclooctadiene (76.8%) cis-cyclooctene (18.9%)
2,5-Norbornadiene	substrate (7.2%) 2-norbornene (68.4%) norbornane (24.4%)	substrate (100%)	
Phenylacetylene	substrate (74.0%) styrene (26.0%)	substrate (95.4%) styrene (4.6%)	
2-Methyl-1-buten-3-yne	substrate (96.8%) isoprene (3.2%)	substrate (100%)	
2-Cyclohexenone	substrate (92.3%) cyclohexanone (6.6%) cyclohexanol (1.1%)	substrate (100%)	
Benzylidenacetone	substrate (80.5%) benzylacetone (19.5%)	substrate (96.9%) benzylacetone (3.1%)	
3-Methyl-2-buten-1-ol		substrate (46.7%) 3-methylbutanol (53.3%)	substrate (79.0%) 3-methylbutanol (21.0%)

[a] Common reaction conditions: solvent = 1,2-dichloroethane (10 ml), T = 353 K, t = 30 min, [**2**] = 8.2×10^{-4} M, [substrate] = 0.210 M.

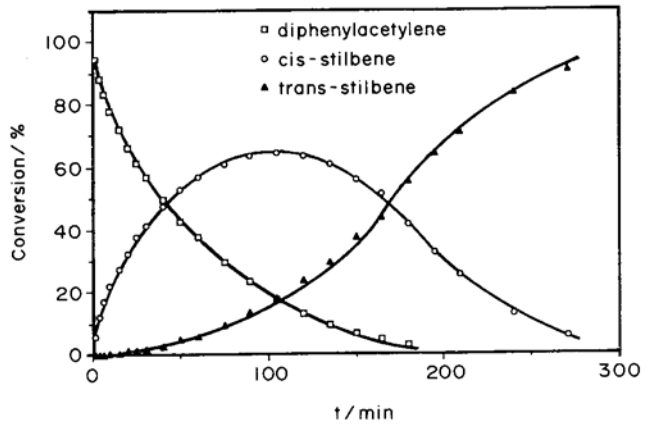

Fig. 5. Catalytic hydrogenation of diphenylacetylene promoted by complex **2** (reaction conditions: $T = 323$ K, 10 ml of 1,2-dichloroethane, $P(H_2) = 0.697$ atm, $[\mathbf{2}]_{t=0} = 8.2 \times 10^{-4}$ M, $[Ph_2C_2]_{t=0} = 0.112$ M).

determine the rate dependence on each reagent, runs were carried out maintaining constant the concentration of the other two reagents (Table 3). The dependence of the rate of dihydrogen consumption on substrate concentration is not linear (Fig. 6), being of positive order at very small substrate concentrations and of nearly zero-order at moderate to high substrate concentrations. Plots of log(rate) vs. log[**2**] and of log(rate) vs. log($P(H_2)$) afford straight lines of slopes 1.09 and 0.96, respectively (Fig. 7), indicating that the reaction is first-order in the concentration of added **2** and in dihydrogen pressure.

Typical substrate saturation kinetics and first-order dependence in catalyst precursor have been reported previously for other cluster-promoted homogeneous hydrogenation reactions in which the nuclearity of the precursor is maintained during the catalytic reaction [13a,15]. Therefore, although we have been unable to isolate or characterize any catalytic intermediates, the kinetic data strongly support the proposition that the catalytic species in the hydrogenation of diphenylacetylene promoted by complex **2** are hexanuclear.

Table 3
Kinetic data for the hydrogenation of diphenylacetylene promoted by complex **2** in 1,2-dichloroethane at 323 K

$P(H_2)$/atm	$[\mathbf{2}] \times 10^4$/M	$[Ph_2C_2]$/M	rate $\times 10^6$/1 s^{-1}
0.275	8.20	0.112	2.80
0.383	8.20	0.112	4.00
0.513	8.20	0.112	4.85
0.697	4.90	0.112	3.30
0.697	8.20	0.112	7.07
0.697	12.30	0.112	10.60
0.697	16.40	0.112	12.30
0.697	8.20	0.014	2.57
0.697	8.20	0.028	5.38
0.697	8.20	0.056	6.46
0.697	8.20	0.168	7.70
0.697	8.20	0.337	9.18
0.697	8.20	0.561	10.40

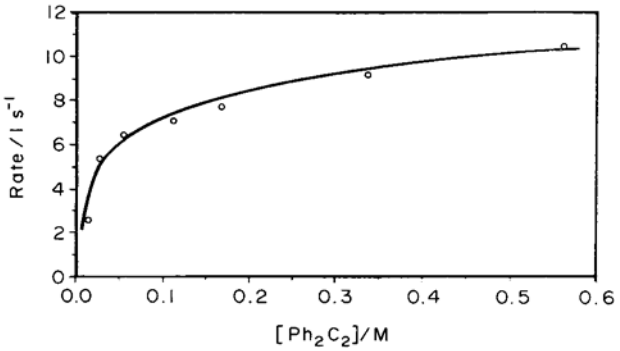

Fig. 6. Plot of the reaction-rate dependence on substrate concentration for the hydrogenation of diphenylacetylene promoted by complex **2**.

3. Experimental details

3.1. General data

Solvents were dried over sodium diphenyl ketyl (THF, diethyl ether, hydrocarbons) or CaH_2 (dichloromethane, 1,2-dichloroethane) and distilled under nitrogen prior to use [16]. The reactions were carried out in

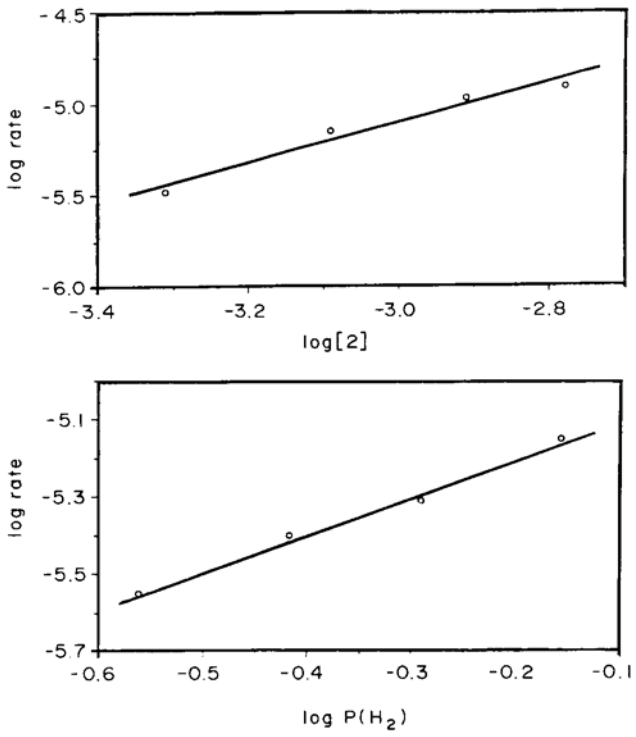

Fig. 7. Partial reaction orders with respect to [**2**] (top) and $P(H_2)$ (bottom) for the hydrogenation of diphenylacetylene promoted by complex **2**.

the absence of air (Schlenk techniques) and were monitored by solution IR spectroscopy (carbonyl-stretching region). Compound **1** was prepared as described previously [17]; a ^{13}CO-enriched sample of compound **1** was prepared from ^{13}CO-enriched $[Ru_3(CO)_{12}]$ [18]. This sample was subsequently used to make ^{13}CO-enriched **2** and **3a**. All other reagents (reagent grade) were used as received from commercial suppliers. Microanalyses were obtained from the University of Oviedo Analytical Service. IR spectra were recorded in solution on a Perkin-Elmer FT 1720-X spectrophotometer, using 0.1 mm CaF_2 cells.

3.2. NMR experiments

^1H, ^{13}C and ^{31}P NMR spectra were run at 23°C in Bruker AC-300 and AMX-400 spectrometers, working at basic frequencies of 300.13 and 400.13 MHz (^1H), 75.5 and 100.62 MHz (^{13}C), and 121.49 and 161.98 MHz (^{31}P), respectively. A 5 mm triple probehead (^1H–^{13}C–^{31}P) was used on the AC-300 spectrometer, affording a 90° pulse width of 12 μs for the ^1H channel, 7 μs for the ^{13}C channel, and 10 μs for the ^{31}P channel. The AMX-400 instrument (UXNMR version 92.08.03) was equipped with a 5 mm reverse BB probehead, giving a pulse duration of 9.6 μs, 12 μs and 16 μs for the ^1H, ^{13}C and ^{31}P nuclei, respectively, at an attenuation level of 3 dB in all cases. Internal $SiMe_4$ (^1H, ^{13}C) or external 85% H_3PO_4 (^{31}P) were used as standards ($\delta = 0$ ppm). A relaxation delay of 2 s was applied in all the experiments.

3.2.1. ^1H NOE-difference spectra of compound 2 (Fig. 3)

Each line of the target multiplet was included in a frequency list and individually pre-irradiated during 0.2 s at a power level of 63 L. The process was repeated cyclicly [19] to afford a saturation period of 7 s. A 90° read pulse yielded the FID, which was exponentially weighted using a line-broadening factor of 0.3 Hz.

3.2.2. ^1H NOESY spectrum of complex 3a (Fig. 4)

The basic pulse sequence of Jeener et al. [20] was used, including TPPI to yield pure absorption signals [21]. The most significant parameters used were as follows: sweep width = 12500 Hz; size in F2 = 1 K; number of increments = 300; zero filling to afford a final matrix of 2048 × 1024 data points; number of scans = 64; mixing time = 0.7 s; apodization in both dimensions by square sinus bell function of $\pi/2$. The obtained spectrum is consistent with the NOE-difference spectra of compound **2**.

3.2.3. ^1H–^{13}C correlations

The indirect detection HMQC experiment [22] was applied. The delay following the first 90° proton pulse was set to a value of 60 ms in order to obtain magnetization derived from heteronuclear long-range couplings. The observed frequencies were restricted to the hydrido and carbonyl regions of the ^1H and ^{13}C NMR spectra, respectively. ^{13}CO-enriched samples were used. Typical parameters were: sweep width = 2800 Hz in F2 and 2000 Hz in F1; size in F2 = 1 K; number of increments = 128; zero filling in F1 up to 1 K; number of scans = 512; weighting function = sinus bell of factor zero in both dimensions; magnitude mode processing. These experiments allowed the asignment of nearly all carbonyl resonances.

3.3. Synthesis of complex 2

Dihydrogen was bubbled through a toluene solution (50 ml) of complex **1** (100 mg, 0.150 mmol) at reflux temperature for 75 min. The solvent was removed under reduced pressure and the residue washed with a mixture of THF (2 ml) and hexane (20 ml), and then with pure hexane (2 × 10 ml), to give complex **2** as a red-brown solid (60 mg, 65%). Anal. Found: C, 25.38; H, 1.77; N, 4.79. $C_{26}H_{20}N_4O_{14}Ru_6$ calc.: C, 25.62; H, 1.65; N, 4.60%. IR (THF): 2063 (s), 2039 (s), 2003 (vs), 1981 (sh), 1941 (w) cm^{-1}. The ^1H and ^{13}C NMR asignments given below (labelling as for **3a** in Fig. 2) are based on ^1H NOE and ^{13}C–^1H correlation experiments. ^1H NMR (THF-d_8): 7.46 (t, $J = 7.8$ Hz, 1 H), 6.84 (d, $J = 7.8$ Hz, 1 H), 6.80 (d, $J = 7.8$ Hz, 1 H), 6.17 (s, NH, H^4), 1.62 (s, ampy Me), −10.84 (m, H^2), −13.53 (m, H^1), −16.74 (m, H^3). $^{13}C\{^1H\}$ NMR (THF-d_8, ^{13}CO-enriched sample): δ(CO) 205.1 (C^6), 200.4 (C^1 or C^3), 200.3 (C^1 or C^3), 200.1 (C^2), 199.1 (C^4 or C^5), 193.8 (C^4 or C^5), 188.6 (C vs. P) ppm.

3.4. Synthesis of complexes 3a and 3b

A THF solution (15 ml) of P(4-tolyl)$_3$ (15.3 mg, 0.050 mmol) and complex **2** (30 mg, 0.025 mmol) was stirred at room temperature for 3 h. The solution was evaporated to dryness under reduced pressure and the residue washed with hexane (2 × 6 ml) to give complex **3a** as a red solid (23 mg, 53%). Anal. Found: C, 44.84; H, 3.99; N, 3.48. $C_{66}H_{62}N_4O_{12}P_2Ru_6$ calc.: C, 44.75; H, 3.53; N, 3.16%. IR (THF): 2027 (s), 2014 (vs), 1980 (m), 1973 (m), 1925 (w) cm^{-1}. $^{31}P\{^1H\}$ NMR (CD_2Cl_2): 26.0 (s) ppm. ^1H NMR (CD_2Cl_2): 7.8–6.8 (m), 6.72 (d, $J = 7.5$ Hz, 1 H), 6.24 (d, $J = 7.5$ Hz, 1 H), 5.87 (s, NH, H^4), 2.34, (s, 4-tolyl Me), 1.55 (s, ampy Me), −10.82 (s, br, H^2), −13.16 (d, br, $J = 19.3$ Hz, H^1), −16.21 (s, br, H^3) ppm. $^{13}C\{^1H\}$ NMR (THF-d_8, ^{13}CO-enriched sample): δ(CO) 207.0 (C^6), 206.5 (C^2), 205.2 (C^1), 201.1 (C^3), 200.9 (C^4), 195.8 (C^5) ppm.

Complex **3b** was prepared in 54% yield by using the same synthetic procedure. Anal. Found: C, 43.33; H, 2.97; N, 3.30. $C_{60}H_{50}N_4O_{12}P_2Ru_6$ calc.: C, 42.71; H,

2.99; N, 3.32%. IR (THF): 2030 (s), 2016 (vs), 1981 (m), 1974 (m), 1928 (w) cm^{-1}. $^{31}P\{^1H\}$ NMR (C_6D_6): 28.9 (s) ppm. ^1H NMR (C_6D_6): 7.9–6.6 (m), 6.39 (t, $J = 7.5$ Hz, 1 H), 6.27 (s, NH, H^4), 6.02 (d, $J = 7.5$ Hz, 1 H), 5.52 (d, $J = 7.5$ Hz, 1 H), 1.82 (s, ampy Me), −10.19 (s, br, H^2), −12.76 (d, br, 21.7 Hz, H^1), −15.61 (s, br, H^3) ppm.

3.5. Catalytic hydrogenation reactions promoted by complex 2

The reactions performed at $P(H_2) > 1$ atm (Table 2) were carried out in a Berghof autoclave. The reactions performed at $P(H_2) = 1$ atm (Table 2) were carried out in the system described below for the kinetic experiments. In all cases, the following reaction conditions were used: solvent = 1,2-dichloroethane (10 ml), T = 353 K, $t = 30$ min, $[\mathbf{2}] = 8.2 \times 10^{-4}$ M, [substrate] = 0.210 M. The products were analyzed by gas chromatography with a Perkin-Elmer 8600 gas chromatograph, equipped with a 30 m Supelcowax-10™ capillary column (i.d. 0.25 mm) and a flame ionization detector; quantification was achieved with a PE-Nelson 1020 integrator.

3.6. Kinetics of the low-pressure catalytic hydrogenation of diphenylacetylene promoted by complex 2

The appropriate amounts of diphenylacetylene and complex **2** (Table 3) were placed in a two-necked 25 ml flask with one neck connected to a gas burette, which in turn was connected to a vacuum line. The flask was closed by a silicone septum and the system evacuated and filled with dihydrogen five times. Dihydrogen-saturated 1,2-dichloroethane (10 ml) was then injected into the flask through the silicone septum and the required pressure adjusted in the gas burette. The flask was immersed in a bath thermostated at 323 K and shaken by a vibrating shaker during the run at 600 shakes min^{-1}. An equilibration time of 2 min was allowed before acquiring any data. The working partial pressure of dihydrogen was determined by subtracting the solvent vapour pressure at 323 K from the measured total pressure. Reactions rates were obtained by measuring the dihydrogen consumption (corrected to 1 atm) in the gas burette as a function of time.

3.7. X-Ray structure determination of $3a \cdot 2CH_2Cl_2$

A dark-red crystal of poor quality, grown at −20°C in the interface of a pentane layer placed on a CH_2Cl_2 solution of the complex, was used for the X-ray diffraction study. The X-ray diffraction data were obtained with an Enraf-Nonius CAD4 diffractometer. A selection of crystal and refinement data is given in Table 4.

Table 4
Selected crystallographic and refinement data for $\mathbf{3a} \cdot 2CH_2Cl_2$

Formula	$C_{66}H_{62}N_4O_{12}P_2Ru_6 \cdot 2CH_2Cl_2$
Formula weight	1941.46
Crystal system	monoclinic
Space group	$P2_1/c$
a, Å	11.939(2)
b, Å	11.964(8)
c, Å	18.19(1)
β, °	116.42(6)
V, Å^3	3778(5)
Z, formula units per cell	2
$F(000)$	1920
D_c, g cm^{-3}	1.71
Crystal size, mm	0.20×0.11×0.13
Radiation (λ, Å)	Mo–Kα (0.71073)
Monochromator	graphite
μ (Mo–Kα), cm^{-1}	13.9
T, K	200
Scan method	ω–2θ
h, k, l range	−21–21, 0–14, 0–21
2θ limits, °	2–50
Total reflections	7437
Unique reflections	6594
Reflections with $I \geq 3\sigma(I)$	2952
Variables	451
$R(F)$	0.049
$R_w(F)$	0.046
$(\Delta/\sigma)_{max}$	0.50
max, min $\Delta\rho$, e Å^{-3}	0.58, −0.62

The unit cell dimensions were determined from the angular settings of 25 reflections with θ between 10 and 15°. The space group was determined to be $P2_1/c$ from systematic absences. The intensity data were measured using the ω–2θ scan technique and a variable scan rate with a max scan time of 60 s per reflection. The intensity of the primary beam was checked throughout the data collection by monitoring three stan-

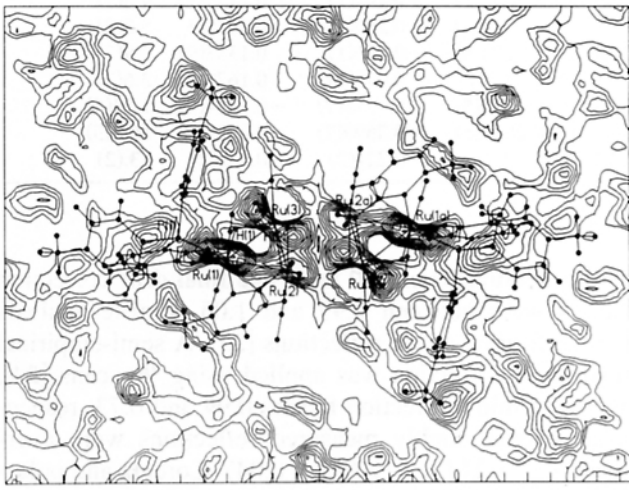

Fig. 8. Difference Fourier synthesis map for $\mathbf{3a} \cdot 2CH_2Cl_2$ excluding the hydrides H(3) and H(3′).

Table 5
Fractional atomic coordinates and equivalent isotropic thermal factors for the non-H atoms of **3a**·$2CH_2Cl_2$

Atom	x	y	z	U_{eq} ($\times 100$ Å^2)
Ru1	0.16752(6)	0.18144(9)	0.18760(7)	2.54(5)
Ru2	0.01977(6)	0.10944(9)	0.10000(7)	2.71(5)
Ru3	0.12533(7)	0.01519(9)	0.05161(7)	2.76(5)
P1	0.3031(2)	0.2079(3)	0.2350(2)	2.7(1)
N1	0.1299(6)	0.3070(8)	0.0881(6)	2.9(5)
N2	0.0526(7)	0.1585(9)	0.0075(7)	3.0(5)
C1	0.1799(8)	0.061(1)	0.2561(9)	3.7(7)
O1	0.1888(6)	−0.0107(9)	0.3008(7)	6.1(5)
C2	0.1402(8)	0.267(1)	0.2581(9)	4.3(7)
O2	0.1226(6)	0.313(1)	0.3012(6)	6.1(6)
C3	0.0048(8)	0.052(1)	0.1884(9)	3.7(7)
O3	−0.0073(7)	0.019(1)	0.2389(7)	7.5(6)
C4	−0.0218(9)	0.246(1)	0.1128(9)	3.9(7)
O4	−0.0441(7)	0.325(1)	0.1254(8)	7.7(7)
C5	0.1841(7)	0.032(1)	−0.0073(9)	3.0(6)
O5	0.2170(6)	0.041(1)	−0.0444(6)	6.0(6)
C6	0.1768(8)	−0.122(1)	0.1022(9)	4.1(7)
O6	0.2026(7)	−0.2018(9)	0.1316(8)	7.0(6)
C7	0.1522(9)	0.416(1)	0.0947(9)	4.2(7)
C8	0.1909(9)	0.468(1)	0.1773(8)	4.6(7)
C9	0.1311(9)	0.480(1)	0.0252(9)	5.1(8)
C10	0.090(1)	0.434(1)	−0.053(1)	7.(1)
C11	0.065(1)	0.327(1)	0.0578(9)	5.6(8)
C12	0.0844(8)	0.267(1)	0.0136(9)	3.8(7)
C13	0.3353(7)	0.297(1)	0.1747(8)	3.2(6)
C14	0.3970(7)	0.371(1)	0.2095(8)	3.2(6)
C15	0.4190(9)	0.434(1)	0.1602(9)	4.3(7)
C16	0.3810(9)	0.428(1)	0.0760(9)	3.7(7)
C17	0.405(1)	0.496(1)	0.022(1)	6.3(9)
C18	0.3165(9)	0.355(1)	0.0403(9)	4.3(7)
C19	0.2939(8)	0.291(1)	0.0892(8)	3.6(6)
C20	0.3634(8)	0.256(1)	0.3398(8)	2.7(6)
C21	0.3339(8)	0.326(1)	0.3784(8)	3.7(6)
C22	0.3786(8)	0.370(1)	0.4539(9)	3.9(6)
C23	0.4576(8)	0.341(1)	0.4962(8)	3.6(7)
C24	0.5063(8)	0.384(1)	0.5822(8)	5.1(7)
C25	0.4869(8)	0.269(1)	0.4592(9)	4.5(7)
C26	0.4409(8)	0.226(1)	0.3823(9)	3.9(7)
C27	0.3469(7)	0.073(1)	0.2319(8)	3.3(6)
C28	0.3524(8)	−0.009(1)	0.2884(9)	4.1(7)
C29	0.3745(8)	−0.120(1)	0.2800(9)	4.2(7)
C30	0.3881(8)	−0.147(1)	0.2133(9)	4.0(7)
C31	0.4064(9)	−0.266(1)	0.202(1)	5.3(8)
C32	0.3824(8)	−0.065(1)	0.1583(9)	3.9(7)
C33	0.3648(8)	0.045(1)	0.1678(8)	3.6(7)
Cl1	0.2753(5)	−0.1598(7)	−0.1454(6)	17.4(6)
Cl2	0.2512(5)	−0.2695(7)	−0.0257(5)	16.8(5)
C101	0.202(1)	−0.224(2)	−0.132(2)	13.(2)

dard reflections every 60 min. The final drift correction factors were between 0.99 and 1.05. Profile analysis was performed on all reflections [23]. A semi-empirical absorption correction was applied using Ψ scans [24], max. and min. correction factors 0.99 and 0.73, respectively. Some doubly measured reflections were averaged, $R_{int} = \Sigma(I - \langle I \rangle / \Sigma I = 0.047$. Lorentz and polarization corrections were applied and the data were reduced to $|F_0|$ values.

The structure was solved by Patterson methods using SHELXS86 [25] and expanded by DIRDIF [26]. Isotropic least-squares refinement, using SHELX76 [27], converged to $R = 0.113$. At this stage, an additional absorption correction was applied using DIFABS [28], max. and min. correction factors 1.18 and 0.59, respectively. The hydrogen atoms except for the bridging hydrido ligands were geometrically placed. In the final stages of the refinement, the positional and anisotropic thermal parameters of the non-H atoms were refined. The hydrogen atoms of the organic ligands were isotropically refined with a common thermal parameter. A different thermal parameter was used for the hydrogen atoms of the solvent molecule. The positions of the hydride ligands were determined from a difference Fourier synthesis and were refined isotropically. Those of H(1) and H(2) refined well, but the position of H(3) was slightly sensitive to the weighting scheme used and therefore the coordinates given for H(3) may not be very accurate. In fact, the identification of hydride H atom positions in a large structure with poor quality data has to be regarded with caution, but nevertheless the positions obtained for the hydrides of **3a** (Fig. 8) have to be close to the real ones because they are consistent with the NMR data. The function minimized was $\Sigma w(F_0 - F_c)^2$, $w = 1/[\sigma^2(F_0) + 0.00025F_0^2]$ with $\sigma(F_0)$ from counting statistics. The atomic scattering factors were taken from ref. [29]. The geometrical calculations were made with PARST [30]. The crystallographic plots were made with the EUCLID package [31]. All calculations were carried out on a Micro VAX-3400 computer at the Scientific Computer Centre of the University of Oviedo. Final atomic coordinates are given in Table 5. Full crystallographic data have been deposited with the Cambridge Crystallographic Data Centre.

Acknowledgements

We thank the CICYT and DGICYT (Spain, Projects MAT90-0173 and PB92-1007) for financial support, the FICYT-Asturias for a postgraduate scholarship (to A.L.), Drs J.F. Van der Maelen and S. García-Granda for the X-ray diffraction data, and Dr F. López-Ortiz for running many NMR spectra.

References

[1] See, for example: (a) D.F. Shriver, H.D. Kaesz and R.D. Adams (eds.), *The Chemistry of Metal Cluster Complexes*, VCH, New York, 1990; (b) M. Moskovits (ed.), *Metal Clusters*, Wiley, New York, 1986.

[2] For relevant reviews on metal clusters in homogeneous catalysis, see: (a) W.L. Gladfelter and K. Roesselet, in ref. [1], Ch. 7, p. 329; (b) G. Süss-Fink and G. Meister, *Adv. Organomet.*

Chem., 35 (1993) 41; (c) L.N. Lewis, *Chem. Rev., 93* (1993) 2693; (d) B.C. Gates, *Catalytic Chemistry*, Wiley, New York, 1992.

[3] J.A. Cabeza, J.M. Fernández-Colinas, A. Llamazares and V. Riera, *J. Mol. Catal., 71* (1992) L7.

[4] J.A. Cabeza, J.M. Fernández-Colinas, S. García-Granda, A. Llamazares, F. López-Ortiz, V. Riera and J.F. Van der Maelen, *Organometallics, 13* (1994) 426.

[5] See, for example: (a) J.A. Cabeza, A. Llamazares, V. Riera, S. Triki and L. Ouahab, *Organometallics, 11* (1992) 3334; (b) J.A. Cabeza, S. García-Granda, A. Llamazares, V. Riera and J.F. Van der Maelen, *Organometallics, 12* (1993) 157; (c) J.A. Cabeza, S. García-Granda, A. Llamazares, V. Riera and J.F. Van der Maelen, *Organometallics, 12* (1993) 2973.

[6] The average Ru–Ru distance in $[Ru_3(CO)_{12}]$ is 2.855 Å: M.R. Churchill, F.J. Hollander and J.P. Hutchinson, *Inorg. Chem., 16* (1977) 2655.

[7] D. Neuhaus and M. Williamson, *The Nuclear Overhauser Effect in Structural and Conformational Analysis*, VCH, New York, USA, 1989, ch. 3, p. 63.

[8] S.A.R. Knox, J.W. Koepke, M.A. Andrews and H.D. Kaesz, *J. Am. Chem. Soc., 97* (1975) 3942.

[9] S.A. MacLaughlin, A.J. Carty and N.J. Taylor, *Can. J. Chem., 60* (1982) 87.

10] For selected reactivity of this complex, see: (a) S.A. MacLaughlin, N.J. Taylor and A.J. Carty, *Inorg. Chem., 22* (1983) 1409; (b) S.A. MacLaughlin, N.J. Taylor and A.J. Carty, *Organometallics, 3* (1984) 392; (c) F. Van Gastel, N.J. Taylor and A.J. Carty, *Inorg. Chem., 28* (1989) 384.

11] M. Castiglioni, R. Giordano and E. Sappa, *J. Organomet. Chem., 362* (1989) 399.

12] See, for example: (a) P.A. Chaloner, M.A. Esteruelas, F. Joó and L.A. Oro, *Homogeneous Hydrogenation*, Kluwer, Dordrecht, 1994; (b) G.W. Parshall and S.D. Ittel, *Homogeneous Catalysis: The Applications and Chemistry of Catalysis by Soluble Transition-Metal Complexes*, Wiley, New York, 1992.

13] (a) J.A. Cabeza, J.M. Fernández-Colinas, A. Llamazares and V. Riera, *Organometallics, 12* (1993) 4141; (b) S. Alvarez, P. Briard, J.A. Cabeza, I. del Río, J.M. Fernández-Colinas, F. Mulla, L. Ouahab and V. Riera, *Organometallics, 13* (1994) 4360; (c) J.A. Cabeza, J.M. Fernández-Colinas, A. Llamazar and V. Riera, *Organometallics, 13* (1994) 4352.

[14] See, for example: (a) R.M. Laine, *J. Mol. Catal., 14* (182) 13 J.A. Cabeza, J.M. Fernández-Colinas, A. Llamazares and Riera, *Organometallics, 11* (1992) 4355.

[15] Y. Doi, K. Koshizuka and T. Keii, *Inorg. Chem., 21* (198 2732.

[16] D.D. Perrin, W.L.F. Armarego and D.R. Perrin, *Purification Laboratory Chemicals*, 2nd ed., Pergamon, Oxford, 1980.

[17] P.L. Andreu, J.A. Cabeza, V. Riera, Y. Jeannin and D. Migu *J. Chem. Soc., Dalton Trans.*, (1990) 2201.

[18] P.L. Andreu, J.A. Cabeza, D. Miguel, V. Riera, M.A. Villa a S. García-Granda, *J. Chem. Soc., Dalton Trans.*, (1991) 533.

[19] M. Kinns and J.K.M. Sanders, *J. Mag. Reson., 56* (1984) 51

[20] J. Jeener, B.H. Meier, P. Bachmann and R.R. Ernst, *J. Che Phys., 71* (1979) 4546.

[21] D. Marion and K. Wuthrich, *Biochem. Biophys. Resp. Commu 113* (1983) 967.

[22] A. Bax, R.H. Griffey and B.L. Hawkins, *J. Mag. Reson.,* (1983) 301.

[23] M.S. Lehman and F.K. Larsen, *Acta Crystallogr., A30* (197 580; D.F. Grant and E.J. Gabe, *J. Appl. Crystallogr., 11* (197 114.

[24] A.C.T. North, D.C. Phillips and F.S. Mathews, *Acta Crysta logr., A24* (1968) 351.

[25] G.M. Sheldrick, in G.M. Sheldrick, C. Kruger and R. Godda (eds.), *Crystallographic Computing 3*, Clarendon, Oxford, 198

[26] P.T. Beurskens, G. Admiraal, G. Beurskens, W.P. Bosman, García-Granda, R.O. Gould, J.M.M. Smits and C. Smykall *The DIRDIF Program System*, Crystallography Laboratory, Ur versity of Nijmegen, Nijmegen, 1992.

[27] G.M. Sheldrick, *SHELX76, Program for Crystal Structure Dete mination*, University of Cambridge, Cambridge, 1976; J.F. V der Maelen, *PhD Thesis*, University of Oviedo, Oviedo, 199

[28] N. Walker and D. Stuart, *Acta Crystallogr., A39* (1983) 158.

[29] *International Tables for X-Ray Crystallography*, Vol. 4, Kynoc Birmingham, 1974.

[30] M. Nardelli, *Comput. Chem., 7* (1983) 95.

[31] A.L. Spek, in D. Sayre (ed.), *Computational Crystallograph* Clarendon, Oxford, 1982, p. 528.